LRP 497/94 September 1994

# VISIBLE PHOTOLUMINESCENCE FROM HYDROGENATED SILICON PARTICLES SUSPENDED IN A SILANE PLASMA

C. Courteille, J.-L. Dorier, J. Dutta.
Ch. Hollenstein, A.A. Howling & T. Stoto

C R P P

ÉCOLE POLYTECHNIQUE FÉDÉRALE DE LAUSANNE - SUISSE

LRP 497/94 September 1994

# VISIBLE PHOTOLUMINESCENCE FROM HYDROGENATED SILICON PARTICLES SUSPENDED IN A SILANE PLASMA

C. Courteille, J.-L. Dorier, J. Dutta,
Ch. Hollenstein, A.A. Howling & T. Stoto

# Visible photoluminescence from hydrogenated silicon particles suspended in a silane plasma

C. Courteille, J.-L. Dorier, J. Dutta, Ch. Hollenstein, and A. A. Howling

Centre de Recherches en Physique des Plasmas,
Ecole Polytechnique Fédérale de Lausanne,
Av. des Bains 21, CH-1007 Lausanne, Switzerland

T. Stoto[a)]

Institut de Genie Atomique,
Ecole Polytechnique Fédérale de Lausanne,
CH-1015 Lausanne, Switzerland

## ABSTRACT

Visible photoluminescence at room temperature has been observed in amorphous hydrogenated silicon particulates during their formation in a silane radio-frequency plasma. Oxygen injection along with mass spectrometry measurements demonstrate that oxygen has no influence on the photoluminescence. The appearance of visible photoluminescence coincides with a particle agglomeration phase as shown by laser light scattering experiments, and electron microscopy shows silicon nanocrystals within these particulates. These observations of visible photoluminescence are consistent with the model of quantum confinement in the silicon nanocrystals.

PACS numbers: 52.80.-s, 52.70.-m, 81.15.Gh, 78.55.-m

a)Present address: Industrial Research Ltd, P.O. Box 31-310, Lower Hutt, New Zealand.

## 1. INTRODUCTION

Micro-particles in reactive gas plasmas are a source of contamination in plasma processing for the micro-electronics industry.[1] Conversely, this environment could be exploited for the production of nano-powders with new properties and potential applications, for example, in the fields of opto-electronics, ceramics, and cluster physics.

In this article we report measurements of photoluminescence (henceforth referred to as PL) during the formation of particulates in a silane plasma. Depending on the plasma parameters, the formation process can occur gradually over many seconds[2-4] to yield particulates up to 0.3 μm diameter for our conditions. Theory[5] and experiment[6] indicate that this plasma polymerisation progresses via negative ion clusters which are trapped by the plasma sheaths and hence have a long lifetime for growth.

Visible PL in porous silicon and silicon particulates is of interest because of the potential application in opto-electronic devices and compatibility with silicon microcircuits. Crystalline silicon is an indirect bandgap material with 1.1 eV optical gap and thus photoluminesces only in the infrared with very weak intensity at room temperature; visible PL in silicon is often associated with polymeric forms of silicon with oxygen[7,8] or quantum confinement in silicon nanostructures.[9] The aim of this study was to observe the development of photoluminescence in free-standing particles as their dimensions increased from macromolecular clusters up to microparticles. This experiment also investigates the feasibility of using photoluminescence as a nanoparticle diagnostic in plasma processing systems.

Any subsidiary effects due to atmospheric exposure or incorporation in a matrix are avoided by performing *in situ* light scattering measurements during growth and suspension in the plasma. Mass spectrometry is used to make quantitative in-process measurements of the effect of oxygen. All stages of preparation are carried out at room temperature; the low-temperature plasma is known not to heat either the gas or the particles significantly.[10] The particle properties have also been measured *ex situ* by electron microscopy, electron diffraction, Raman scattering, and IR absorption.[11]

## 2. EXPERIMENTAL APPARATUS

The apparatus is a conventional capacitively-coupled parallel-plate reactor with 130 mm diameter electrodes, described in detail elsewhere.[12] Pure silane was used at a flow rate of 30 sccm and 0.1 mbar pressure. The whole reactor was at room temperature to give a high powder yield[13] and to avoid thermophoresis forces[14] from temperature gradients. Clouds of powder form 5 to 60 s after ignition (depending on the plasma parameters) and are suspended in the plasma.[2,3,15] These were irradiated by an unfocused argon ion laser (3 mm beam diameter) operating either at 488 nm (through a 9 nm width bandpass filter) or in the UV range (351 and 364 nm) with a 0.1 - 1 W range of continuous power. The PL signal was observed perpendicularly to the laser beam through a lens using an appropriate high-pass filter to remove laser light elastically-scattered from the powder particles (Fig. 1). The measured spectra were corrected for the spectral response of the detection system calibrated with a tungsten filament standard source. A mass spectrometer[16] was mounted in the ground electrode for simultaneous measurement of the positive ion flux from the plasma.

The rf power was on/off modulated at 20 kHz and a synchronously-gated optical multichannel analyser (OMA) and monochromator were used to monitor the PL (Fig. 1). The excitation frequency was 30 MHz at a time-averaged input power of 3 to 10 W. All plasma emission decayed away 5 μs into the afterglow, and the PL was acquired after this time during the afterglow to avoid any contribution from the plasma emission (there was no signal with the laser off). The OMA gate duration was typically 15 μs per cycle for 66 000 cycles. The 20 kHz square-wave modulation frequency was chosen because the powder production rate was sufficiently high and gave a uniform distribution of powder all along the laser beam path between the electrodes.

## 3. RESULTS

### 3.1 Photoluminescence spectra in steady-state conditions

After the powder has formed, illumination with the UV laser wavelength shows PL clearly visible to the naked eye in the plasma as a luminous reddish-white line along the laser path: the PL intensity is strong compared to the blue plasma glow (414 nm SiH molecular band

emission). For the green/blue laser line at 488 nm, a high pass filter is necessary to remove the elastically-scattered light for the PL to be visible by eye. Significant portions of the spectra shown in Fig. 2 are in the visible region, especially when using UV irradiation. The shift in the PL spectrum with laser wavelength is due to excitation of higher energy states by the UV (3.5 eV) radiation which are inaccessible at 488 nm (2.5 eV). With the quantum confinement interpretation, this suggests that different sizes of nanocrystals are simultaneously present. This is consistent with Raman scattering measurements[11] and is probably the reason for the broad PL spectra observed (further results are reported in Sections 3.3 and 3.4).

It is important to consider whether the laser perturbs the plasma or the particles. For the argon ion laser power range used here, the PL intensity increased monotonically (sublinear) with power. Different experiments with high power (> 5 $MWcm^{-2}$) pulsed lasers are known to perturb the discharge chemistry[17] and evaporate the particles.[18] However, simultaneous monitoring of the particles using a low power HeNe laser arranged co-linearly (see Fig. 1) with the argon ion laser, at either the 488 nm or UV wavelengths, showed no change in the HeNe light scattered from the powder when the argon ion laser was switched on or off. We deduce that the argon ion laser is not influencing the particle sizes or number density in the plasma.

Particle incandescence due to laser heating as an emission source can be excluded since the temperature corresponding to the observed peak intensity at around 900 nm would be 3200 K by Wien's law (2700 K accounting for size effects[19]), too high for the particles to exist. Moreover, the spectral form is invariant over at least an order of magnitude of the laser power and is in any case incompatible with a blackbody spectrum. Sources of emission other than PL can therefore be discounted.

### 3.2 *Insensitivity of the photoluminescence to oxygen*

Oxygen-containing compounds such as siloxene and its derivatives have been proposed to be at the origin of visible PL in porous silicon.[7,8,20] In the literature, thermal oxidation or exposure of samples to atmosphere makes the rôle of oxygen difficult to determine unambiguously. Our powder samples readily oxidize upon exposure to air[11] and even residual oxygen in the vacuum system could be sufficient to partially oxidise the samples[21] since any

oxygen is scavenged by reactions with the particles. It is therefore impractical to eliminate oxygen entirely and instead we added a small flow (up to 1 sccm) of oxygen to the silane plasma and tested whether the PL intensity increased accordingly.

The oxygen was introduced via a calibrated needle valve mounted directly on the vacuum chamber, and a mass spectrometer[16] in the ground electrode (Fig. 1) was used to make quantitative in-process measurements of the oxygen content of positive ions in the plasma. Mass spectrometry rather than optical spectroscopy of the plasma emission was chosen as an appropriate diagnostic for this application because the oxygen did not exist as a free excited radical in sufficient quantities to be detected optically.

Figure 3(a) shows the mass spectrum of the positive ion flux from a pure silane plasma (30 sccm flowrate) using a degraded mass resolution to enhance sensitivity. The signal is principally due to groups of $Si:H^+$ ions. The peaks are spaced at 28 amu intervals where each peak represents a group of ionic molecules with a given number of silicon atoms (mass 28 amu) irrespective of their hydrogen content. Figure 3(b) shows the positive ions for identical conditions except for the addition of 1 sccm of oxygen. The new intermediate peaks are $Si:O:H^+$ ions (atomic mass 16 amu for oxygen) which now form 30% of the total ion flux whereas previously they were present in only trace quantities in Fig. 3(a). Clearly, the oxygen is efficiently scavenged and forms Si:O:H compounds in the plasma. The powder was continuously monitored with the HeNe laser during oxygen injection: the powder quantity was unaltered and the only effect of the oxygen was to decrease the time of formation of the powder. The added oxygen never increased the PL intensity or changed the form of the PL spectrum, whether the oxygen flow was added to the silane flow before or after plasma ignition.

Comparison of Figs. 3(a) and 3(b) shows that the plasma was certainly not saturated with siloxene-like compounds before adding 1 sccm of oxygen. Therefore the invariance of the PL intensity with added oxygen demonstrates that oxygen plays no rôle in the PL mechanism in this experiment whether via siloxene derivatives, oxides, or surface states involving oxygen.

### 3.3 Development of the photoluminescence during particle growth

In previous studies we measured a sequence of sub-nanometric anionic clusters from silane radicals up to silicon hydride clusters containing many silicon atoms by quadrupole mass spectrometry.[6,22] The largest contained 40 silicon atoms[22] which is estimated to be about 1 nm in diameter. To increase the size range of investigation, the aim was to use PL as a diagnostic for nanometric particles which are too small to be observed by elastic scattering of visible light. Mie scattering (Rayleigh scattering for the limit of particles small compared to the wavelength) is not practical for particles smaller than about 20 to 30 nm diameter for our particle number densities (around $10^8$ to $10^9$ $cm^{-3}$) and laser intensity.

Following the quantum confinement model, calculations[23,24] predict crystal sizes of approximately 1.5 nm for a 3.5 eV effective bandgap and 2 nm for 2.5 eV. Therefore, if the nanocrystals grew gradually with time, the UV laser (3.5 eV) would excite visible PL at an earlier stage in the particle development than the 488 nm wavelength (2.5 eV) radiation.

However, simultaneous observation of growing particles by PL and Mie scattering, using the co-linear UV and HeNe lasers respectively, showed that the PL signal does not precede the HeNe scattering signal although the particle sizes for each observation are widely different (about 1.5 nm and > 20 nm respectively). This was investigated quantitatively using the single argon ion laser at 488 nm wavelength to monitor both the PL and elastically-scattered light; both signals therefore correspond to exactly the same group of particles. Figure 4 compares the time-dependence of the PL with the particle size and number density deduced from analysis of the Mie scattering (see Hollenstein *et al*[4] for a description of the method). The figure shows that no visible PL is observed until an agglomeration phase[3,4] when clusters combine to give particles large enough to scatter visible light. This observation is independent of the presence or absence of added oxygen. The non-detection of PL before agglomeration is not due to a lack of detector sensitivity because the clusters are more numerous before the agglomeration phase (Fig. 4) and furthermore, smaller particles are expected to give more intense PL through stronger quantum confinement effects.[24-26]

We conclude that the visible PL from free-standing silicon hydride nanometric clusters is much weaker than the visible PL from particulates which are themselves much too large to act as single crystals with an enhanced bandgap.

A possible explanation is that *nanocrystals which photoluminesce are formed during the agglomeration phase* and not before. These nanocrystals therefore would not exist in isolation, but form in the amorphous matrix of a particle (see section 3.4 for observations) where host atoms could stabilise the nanocrystal surface by saturating its surface bonds.[25,27] Furthermore, it is known that silicon nanocrystals smaller than about 3 nm can only survive a transition to the amorphous phase if they are embedded in a material which reduces the crystallite size stability limit .[26,28]

### 3.4 Nanocrystals and powder structure using *ex situ* diagnostics

Electron microscopy of the yellow-brown powder collected on a carbon-coated copper grid shows spherical aggregates, up to 300 nm in diameter, of coalesced spheres, like blackberries, whose symmetry suggests that they were formed while suspended in the plasma.[4,11] Within the particles, randomly-distributed nano-sized crystalline islands embedded in an amorphous matrix can be seen by high resolution transmission electron microscopy in Fig. 5, similar to observations in porous silicon.[29,30] This observation is further supported by Raman scattering[11] and selected area electron diffraction in the powder which find a heterogeneous distribution of crystalline and amorphous phases similar to measurements made in porous silicon.[30,31] The Raman measurements[11] also indicate a large range of crystal sizes, consistent with an inhomogeneously-broadened PL spectrum, of average diameter below 10 nm. Raman scattering in porous silicon[32] and nanocrystalline photoluminescent PECVD films[27] estimate an average nanocrystal size of approximately 3 nm.

The observation of nanocrystals is not sufficient to prove that quantum confinement is the origin of the PL, nevertheless it is important corroborative evidence.[27,29-33] Using the results from the previous section, one could speculate that the nanocrystals are formed by quenching or condensation during the agglomeration phase.[34]

## 4. DISCUSSION

The vast majority of visible PL studies are concerned with porous silicon and we now consider our results in this context. Different interpretations for the origin of visible PL in silicon are quantum confinement in nanocrystalline silicon,[9] and oxygen effects via surface oxides or siloxene ($Si_6O_3H_6$) and its derivatives.[7,8,20]

The large specific area of porous silicon and powders implies a sensitivity to physisorbed molecules which can stabilise electrons or holes at the silicon surface.[35,36] This may be responsible for the quenching of PL in silicon powder by gas pressure as observed by Costa *et al* [37] and independently by us. Surface passivation via a good quality silicon dioxide barrier layer on porous silicon gives intense PL.[38,39] Nevertheless, when surface passivation is achieved without relying on an oxide layer, it is found that efficient PL still occurs.[27,40-42] It would appear that the oxide layer is not the origin of the PL, but provides the surface passivation which permits radiative recombination in the crystallites by removing competitive nonradiative relaxation at surface states.[43] The results in Section 3.2 also find that oxygen plays no rôle in the visible PL emission of hydrogenated silicon particles, and so neither oxides nor siloxene are at the origin of this visible PL. Furthermore, PL is not observed in amorphous hydrogenated silicon[29,33] or purely amorphous silicon[32]: some degree of crystallinity is necessary to obtain visible PL.[29,33] PL in siloxene has even been attributed to quantum confinement in silicon nanocrystals.[44]

These PL observations are consistent with quantum confinement in nanocrystals which enhances the band gap of the material and results in a relaxation of the momentum selection rule to allow transitions forbidden in bulk silicon - the nanocrystal becomes a direct bandgap material with consequently higher PL intensity.[24,25] During agglomeration, the host atoms of the amorphous matrix may simultaneously satisfy two conditions: passivation of surface states,[43] and stabilisation of the nanocrystal surface.[25,27]

Future objectives would be to select the nanocrystal size, distribution and volume fraction by controlling the plasma parameters. Nanostructures can be synthesised from macromolecular clusters in plasmas, in ion traps,[45] or directly grown in hydrogenated silicon films.[26,27]

## 5. CONCLUSIONS

Broad spectrum visible photoluminescence is observed at room temperature in hydrogenated silicon particles during suspension in a radio-frequency silane plasma. The photoluminescence appears only after a particle agglomeration phase and does not depend on the presence of oxygen. A large size range of silicon nanocrystals exists, embedded in the amorphous matrix of the particulates. The origin of this photoluminescence is consistent with the model of quantum confinement in the nanocrystals.


## ACKNOWLEDGMENTS

We thank Professor L. Zuppiroli, Dr. Ch. Nieswand and L. Sansonnens for their assistance and encouragement. This work was supported by the Swiss Federal Optics Priority Program and Swiss Federal Grants EF-REN (93)035 and BBW.93.0136 (for Brite-Euram contract BE-7328).

## REFERENCES


[1]G. S. Selwyn, J. S. McKillop, K. L. Haller and J. J. Wu, J. Vac. Sci. Technol. A **8**, 1726 (1990).

[2]A. Bouchoule, A. Plain, L. Boufendi, J. Ph. Blondeau and C. Laure, J. Appl. Phys. **70**, 1991 (1991).

[3]L. Boufendi, A. Plain, J. Ph. Blondeau, A. Bouchoule, C. Laure and M. Toogood, Appl. Phys. Lett. **60**, 169 (1992).

[4]Ch. Hollenstein, J.-L. Dorier, J. Dutta and A. A. Howling, to appear in Pl. Sources, Sci. and Technol.

[5]S. J. Choi and M. J. Kushner, J. Appl. Phys. **74**, 853 (1993).

[6]A. A. Howling, L. Sansonnens, J.-L. Dorier, and Ch. Hollenstein, J. Appl. Phys.**75**, 1340 (1994).

[7]M. S. Brandt, H. D. Fuchs, M. Stutzmann, J. Weber, and M. Cardona, Solid State Commun. **81**, 307 (1992).

[8]M. Stutzmann, J. Weber, M. S. Brandt, H. D. Fuchs, M. Rosenbauer, P. Deák, A. Höpner, and A. Breitschwerdt, Solid State Phys. **32**, 179 (1992).

[9]L. T. Canham, Appl. Phys. Lett. **57**, 1046 (1990).

[10]J. E. Daugherty and D. B. Graves, J. Vac. Sci. Technol. A **11**, 1126 (1993).

[11]J. Dutta, W. Bacsa, and Ch. Hollenstein, submitted to J. Appl. Phys.

[12]J.-L. Dorier, Ch. Hollenstein, A. A. Howling and U. Kroll, J. Vac. Sci. Technol. A **10**, 1048 (1992).

[13]A. M. Wróbel and M. R. Wertheimer, Plasma Deposition, Treatment, and Etching of Polymers, edited by R. d'Agostino (Academic, New York, 1990).

[14]G. M. Jellum, J. E. Daugherty and D. B. Graves, J. Appl. Phys. **69**, 6923 (1991).

[15]A. A. Howling, Ch. Hollenstein, and P.-J. Paris, Appl. Phys. Lett. **59**, 1409 (1991).

[16]Hiden Analytical Limited, Gemini Business Park, Warrington WA5 5TN, UK.

[17]K. G. Spears, T. J. Robinson, and R. M. Roth, IEEE Trans. Plasma Sci. PS-**14**, 179 (1986).

[18]W. W. Stoffels, E. Stoffels, G. M. W. Kroesen, and F. J. De Hoog, J. Appl. Phys. **74**, 2959 (1993).

[19]R. Scholl and B. Weber, NATO ASI Series C, Mathematical and physical sciences; Vol. 374 *Physics and Chemistry of Finite Systems: From Clusters to Crystals* edited by P. Jena, S. N. Khanna and B. K. Rao, (Kluwer Academic Publishers, 1992), Vol. 1 p 1275

[20]P. Deák, M. Rosenbauer, M. Stutzmann, J. Weber, and M. S. Brandt, Phys. Rev. Lett. **69**, 2531 (1992).

[21]Y. Xiao, M. J. Heben, J. M. McCullough, Y. S. Tsuo, J. I. Pankove and S. K. Deb, Appl. Phys. Lett. **62**, 1152 (1993).

[22]C. Courteille, L. Sansonnens, J. Dutta, J.-L. Dorier, Ch. Hollenstein, A. A. Howling, and U. Kroll, Proc. 12th Eur. Photovoltaic Solar Energy Conf., April 1994, Amsterdam, The Netherlands.

[23]J. P. Proot, C. Delerue, and G. Allan, Appl. Phys. Lett. **61**, 1948 (1992).

[24]A. J. Read, R. J. Needs, K. J. Nash, L. T. Canham, P. D. J. Calcott and A. Qteish, Phys. Rev. Lett. **69**, 1232 (1992).

[25]S. Schmitt-Rink, D. A. B. Miller and D. S. Chemla, Phys. Rev. B **35**, 8113 (1987).

[26]M. Rückschloss, B. Landkammer, and S. Veprek, Appl. Phys. Lett. **63**, 1474 (1993).

[27]X. Liu, X. Wu, X. Bao, and Y. He, Appl. Phys. Lett. **64**, 220 (1994).

[28]S. Veprek, Z. Iqbal, and F.-A. Sarott, Philos. Mag. B **45**, 137 (1982).

[29]W. Cao and A. J. Hunt, Appl. Phys. Lett. **64**, 2376 (1994).

[30]M. W. Cole, J. F. Harvey, R. A. Lux, D. W. Eckart, and R. Tsu, Appl. Phys. Lett. **60**, 2800 (1992).

[31]A. Nakajima, Y. Ohshima, T. Itakura, and Y. Goto, Appl. Phys. Lett. **62**, 2631 (1993).

[32]R. Tsu, H. Shen, and M. Dutta, Appl. Phys. Lett. **60**, 112 (1992).

[33]K. H. Jung, S. Shih, D. L. Kwong, C. C. Cho, and B. E. Gnade, Appl. Phys. Lett. **61**, 2467 (1992).

[34]A. Garscadden, NATO ASI Series B: Physics Vol. 220. *Nonequilibrium Processes in Partially Ionised Gases* , edited by M. Capitelli and J. N. Bardsley, (Plenum, New York, 1990), p. 541; and A. Garscadden, Proc. XXth Int. Conf. in Ionised Gases (Pisa), Invited Paper (1991) p147.

[35]J. M. Lauerhaas and M. J. Sailor, Science **261**, 1567 (1993).

[36]M. Ben-Chorin, A. Kux, and I. Schechter, Appl. Phys. Lett. **64**, 481 (1994).

[37]J. Costa, P. Roura, G. Sardin, J. R. Morante and E. Bertran, Appl. Phys. Lett. **64**, 463 (1994).

[38]V. Petrova-Koch, T. Muschik, A. Kux, B. K. Meyer, F. Koch, and V. Lehmann, Appl. Phys. Lett. **61**, 943 (1992).

[39]J. L. Batstone, M. A. Tischler, and R. T. Collins, Appl. Phys. Lett. **62**, 2667 (1993).

[40]S. L. Friedman, M. A. Marcus, D. L. Adler, Y.-H. Xie, T. D. Harris and P. H. Citrin, Appl. Phys. Lett. **62**, 1934 (1993).

[41]A. Grosman, C. Ortega, J, Siejka and M. Chamarro, J. Appl. Phys. **74**, 1992 (1993).

[42]S. Shih, K. H. Jung, D. L. Kwong, M. Kovar, and J. M. White, Appl. Phys. Lett. **62**, 1780 (1993).

[43]H. Morisaki, F. W. Ping, H. Ono and K. Yazawa, J. Appl. Phys. **70**, 1869 (1991).

[44]R. F. Pinizzotto, H. Yang, J. M. Perez, and J. L. Coffer, J. Appl. Phys. **75**, 4486 (1994).

[45]T. Kanayama, private communication.

## FIGURE CAPTIONS

FIG. 1. Schematic plan view of the ground electrode, lasers and light collection system. The argon ion laser beam height is adjusted to intersect the powder suspended in the plasma, with the low power He-Ne laser aligned co-linearly to monitor the Mie scattering from the powder particles. The optical multichannel analyser (OMA) gating relative to the rf power modulation is shown diagrammatically. The mass spectrometer orifice is at the center of the ground electrode.

FIG. 2. Steady-state photoluminescence spectra from the suspended particles irradiated by an argon ion laser separately for the 488 nm wavelength and the UV range (with highpass optical filter edges indicated at 515 nm and 420 nm respectively). The intensities are corrected for the optical system response whose limit for reliable calibration was 850 nm. Time-averaged rf input power 4 W; laser power 1 W.

FIG. 3. Positive ion mass spectra for: (a) silane plasma (30 sccm) showing $Si:H^+$ ions; and (b) the same plasma with 1 sccm of oxygen added. The shaded areas correspond to $Si:O:H^+$ ions. Time-averaged rf input power 3 W.

FIG. 4. Development of particle agglomeration and photoluminescence with time after plasma ignition. (a) Measured intensities of polarised light scattering and transmitted light, compared with a self-consistent fitting procedure(HOLLENSTEIN) used to estimate: (b) particle radius and number density. (c) Simultaneously-measured photoluminescence intensity for the same particles. Time-averaged rf input power 4 W; laser power 1 W.

FIG. 5. Micrograph of a particle measured by high resolution transmission electron microscopy showing nanocrystalline regions.

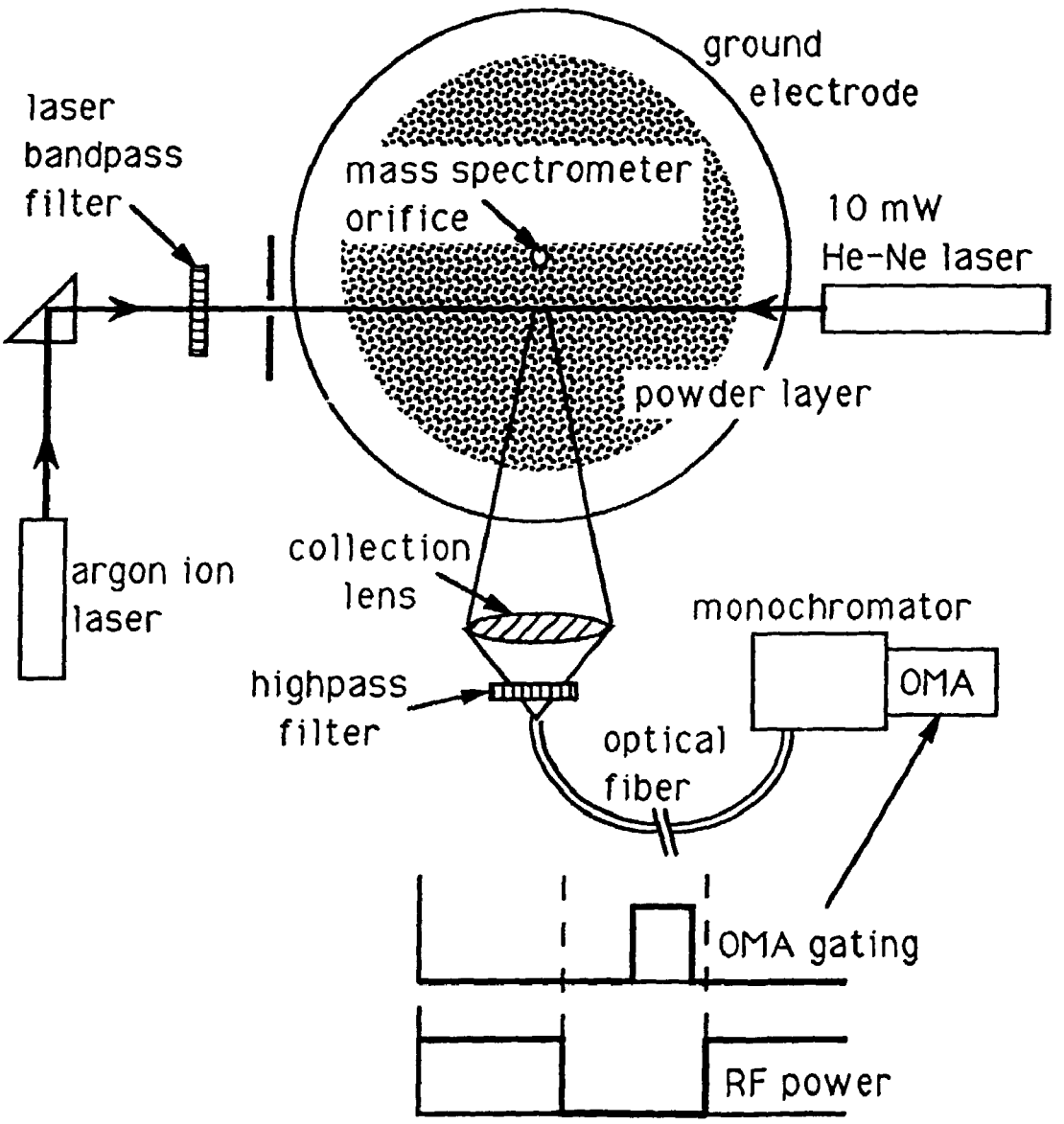
ground
electrode
laser
bandpass
filter
mass spectrometer
orifice
10 mW
He-Ne laser
powder layer
argon ion
laser
collection
lens
monochromator
OMA
highpass
filter
optical
fiber
OMA gating
RF power

Fig. 1

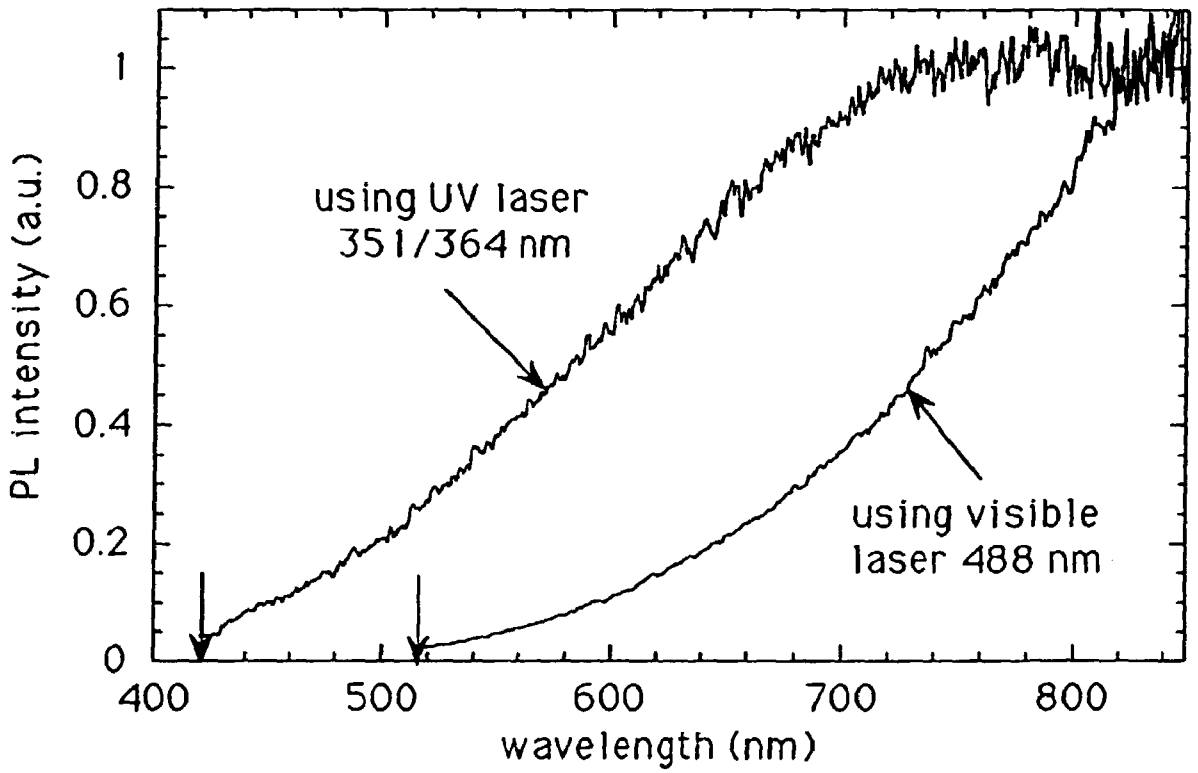
PL intensity (a.u.)
1
0.8
0.6
0.4
0.2
0
400
500
600
700
800
wavelength (nm)
using UV laser
351/364 nm
using visible
laser 488 nm

Fig. 2

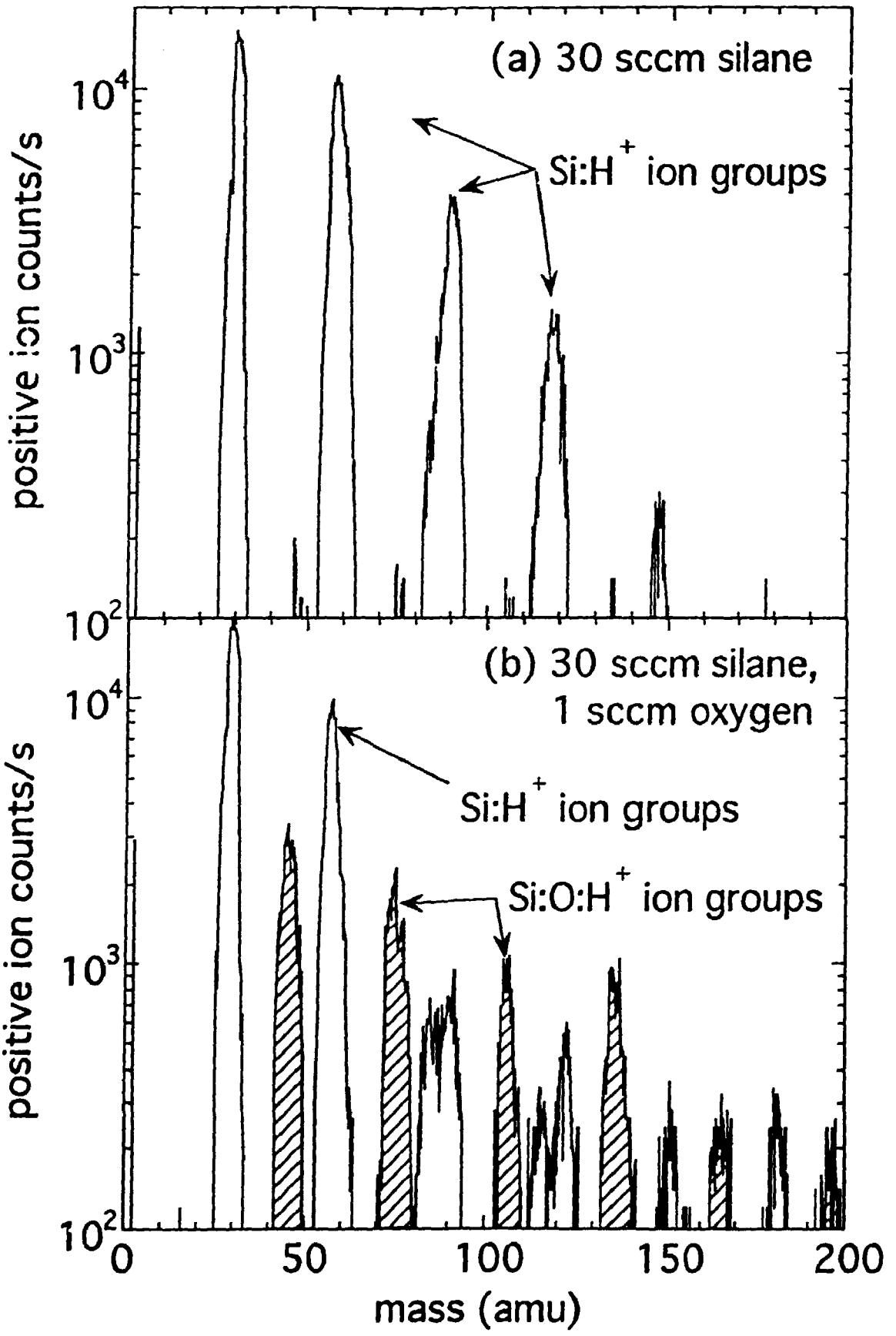
(a) 30 sccm silane
Si:H+ ion groups
positive ion counts/s
10^4
10^3
10^2
(b) 30 sccm silane,
1 sccm oxygen
Si:H+ ion groups
Si:O:H+ ion groups
positive ion counts/s
10^4
10^3
10^2
0
50
100
150
200
mass (amu)

Fig. 3

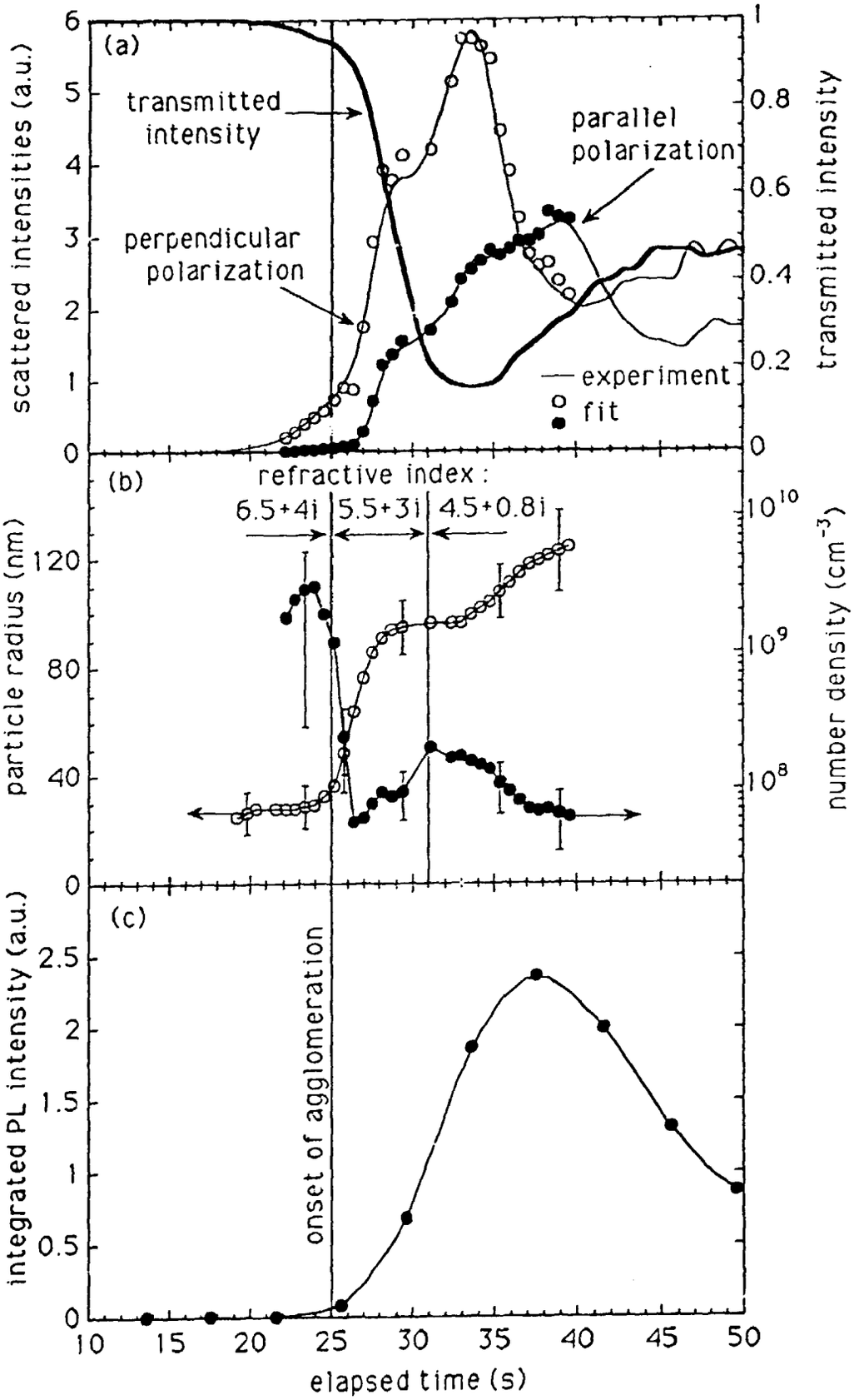
(a)
transmitted intensity
parallel polarization
perpendicular polarization
experiment
fit
scattered intensities (a.u.)
transmitted intensity
(b)
refractive index :
6.5+4i
5.5+3i
4.5+0.8i
particle radius (nm)
number density (cm$^{-3}$)
(c)
onset of agglomeration
integrated PL intensity (a.u.)
elapsed time (s)

Fig. 4


Fig. 5